



Beyond trends and cycles: rainfall as a sequence of irregular regimes

Arianna Di Paola¹, Massimiliano Pasqui¹, Ramona Magno², Sara Quaresima¹, Edmondo Di Giuseppe¹

¹ National Research Council of Italy, Institute of Bioeconomy, Rome, 00185, Italy

⁵ ² National Research Council of Italy, Institute of Bioeconomy, Sesto Fiorentino, 50019, Italy

Correspondence to: Massimiliano Pasqui (massimiliano.pasqui@cnr.it)

Abstract. Rainfall is an oscillatory rather than purely stochastic signal, whose variability reflects alternating hydrological regimes rather than long-term trends. Recognizing this regime-based nature marks a conceptual shift in the way climatology interprets rainfall variability. At the monthly to multiannual scale, precipitation evolves through irregular wet, dry, and 10 stationary phases whose duration and intensity vary over time. Although trend analyses, anomaly-based metrics, and spectral methods may at times suggest contrasting interpretations - each being sensitive to different aspects of the signal - they capture only partial views of a shared underlying variability. Framing precipitation as a sequence of irregular regimes offers a unifying perspective that helps reconcile these approaches and clarifies how rainfall fluctuations actually unfold. Using the Po River basin (Northern Italy) as an illustrative case, we show that Fourier and wavelet analyses confirm the 15 intermittent character of rainfall oscillations, with regular periodicities emerging only at limited intervals. The Cumulative Deviation from Normal (CDN), computed as the cumulative sum of standardized monthly precipitation (SPI1), provides a simple yet physically consistent framework to visualize these irregular regimes and to quantify the resulting changes in water availability driven by cumulative surplus or deficit.

1 Introduction

20 In climatological studies, rainfall variability has long been interpreted in divergent ways. Most applied analyses - typically conducted at monthly or annual scales - treat precipitation as a random variable fluctuating around a long-term mean and evaluate it through linear trends or anomalies relative to its climatology (Vicente-Serrano et al., 2025; Beranová et al., 2025; Luppichini and Bini, 2025; Doane-Solomon et al., 2025). However, extensive empirical evidence suggests that this view captures only part of the phenomenon's complexity.

25 Rainfall is not a purely stochastic process, but an oscillatory signal composed of multiple, irregular, and overlapping fluctuations evolving across time and space. Already in the 1990s, Hu and Nitta (1996) revealed, through wavelet analysis of century-long Asian records, the coexistence of biennial, interannual, and decadal components within the same time series. Subsequent studies (Willems, 2013; Valdés-Pineda et al., 2018; Dieppois et al., 2019; Kim and Ha, 2021) confirmed that 30 precipitation variability is inherently multiscale and modulated by large-scale ocean–atmosphere teleconnections such as El Niño–Southern Oscillation, Pacific Decadal Oscillation, and Atlantic Multidecadal Oscillation. These fluctuations give rise to prolonged wet or dry regimes that can mimic local trends while remaining part of a reversible oscillatory behavior.



Although the oscillatory nature of rainfall is well established in academic literature, it has been only partially incorporated into applied climatology.

35 Recognizing rainfall variability as an expression of irregular and overlapping regimes, yet not regular harmonic cycles, represents both a conceptual and operational step forward. Linear-trend approaches benefit from being simple and reproducible, but they can obscure localized departures - such as multi-year drying or wetting phases - that leave a meaningful imprint within the broader record.

40 For instance, recent studies assessing whether Mediterranean precipitation exhibits a long-term trend have produced apparently contrasting results (Vicente-Serrano et al., 2025; Beranová et al., 2025; Luppichini and Bini, 2025; Doane-Solomon et al., 2025). Some identify statistically significant - usually negative - trends within specific intervals or regions, including those derived from changepoint analyses that detect shifts in level or variability rather than regular periodicities (Mendes et al., 2022; Caloiero et al., 2018). Others, based on longer and more homogeneous records, report overall stationarity of annual totals.

45 Meanwhile, the intermittent expression of regular periodicities makes rainfall's oscillatory behavior more difficult to discern and may help explain why it is often overlooked. However, analytical tools capable of detecting such oscillations - such as wavelet transforms or multifractal decompositions - offer valuable insights but require long, homogeneous time series and substantial mathematical expertise. Even under these conditions, they seldom resolve the direction or phase state of the signal and remain difficult to apply in operational settings. Rainfall regimes remain largely obscured when viewed through methods optimized for trends or regular periodicities, underscoring the need for representations capable of capturing their 50 inherently irregular and overlapping nature.

2 Paradigm Shift

The Cumulative Deviation from Normal (CDN) complements canonical analytical tools, offering a physically consistent and accessible way to describe how precipitation evolves through overlapping, multiscale, and irregular regimes.

55 Conceptually, the CDN represents the cumulative deviation of monthly precipitation from its standardized value, tracing over time the integrated hydrological balance of the system. Cumulative curves of this kind have historically been used in hydrology (Wu et al., 2024; Samil et al., 2019; Weber and Stewart, 2004) to highlight recharge and depletion phases in groundwater and lake levels. Their use, however, has been limited by the appearance of long-term numerical drifts arising from the use of the arithmetic mean as the "normal" reference. In positively skewed distributions such as monthly precipitation, even without zero inflation, about 60% of values fall below the mean, while infrequent extreme events tend to 60 bias the curve toward positive deviations. As a result, the cumulative sum of monthly anomalies progressively diverges from zero, generating artificial long-term trends.

This limitation can be overcome by computing the CDN as the cumulative sum of the 1-month Standardized Precipitation Index (SPI1), where precipitation is first fitted with a gamma distribution and then transformed to a normalized anomaly



with zero mean and unit variance (Di Paola et al., 2025). In this formulation, the CDN gains statistical consistency and filters 65 out short-term stochastic noise in favor of identifying medium- to long-term behavior. It thus becomes a robust tool for visualizing hydrological memory and the sequence of wet, dry, or stationary regimes that would otherwise remain hidden (Fig. 1a and b).

Each ascending or descending segment of the CDN corresponds to a wet or dry regime, respectively, while nearly horizontal 70 sections indicate stationary conditions. The irregular alternation of these segments reveals the episodic, regime-based dynamics of rainfall—intrinsically irregular and therefore difficult to predict deterministically.

Beyond its statistical consistency, the CDN provides an integrated and inherently multiscale view of rainfall variability. By 75 accumulating standardized anomalies, it embeds the contribution of all temporal scales into a single continuous trajectory, revealing hydrological regimes whose phase, duration, amplitude, and overlap are difficult to detect with fixed scales or classical time–frequency tools. This conceptual view is formally derived in Appendix A, where we show that CDN uniquely determines all multiscale SPI aggregates.

3. Illustrative Example: the Po River Basin

3.1 Data and analytical setup

Monthly precipitation data for the Po river basin (1961–2025) originate from the ARCIS dataset (Pavan et al., 2019). Daily values were aggregated into monthly totals and spatially averaged over the entire basin.

80 The resulting series was standardized into the Standardized Precipitation Index (McKee et al., 1993) at the one-month scale (SPI1), to remove seasonality and normalize the positively skewed distribution typical of rainfall. The Cumulative Deviation from Normal (CDN) was then computed as the cumulative sum of SPI1, representing the integrated water-balance anomaly in units of SPI1 standard deviations.

The SPI1 time series was analysed for breakpoints, trends, and periodicity. Significant change points ($\alpha = 0.05$) were tested 85 using the non-parametric Pettitt test (Truong et al., 2020), which detects distributional shifts in the median of a time series without assuming normality. No statistically significant change points were detected. Therefore, the presence of any persistent monotonic trend over the full record (1961–2025) was evaluated using the non-parametric Mann–Kendall test (Mann, 1945), which confirmed the absence of statistically significant trends.

A continuous wavelet transform (CWT) was applied to detect periodic components in the SPI1 signal, following the method 90 of (Torrence and Compo, 1998). The analysis used a Morlet mother wavelet ($\omega_0 = 6$) and a monthly time step ($\Delta t = 1$). Scales ranged from 2 to 240 months with a \log_2 spacing of 1/12. Wavelet power was normalized by scale and tested for significance against a red-noise AR (1) background at the 95% confidence level. The corresponding Fourier power spectral density (Youngworth et al., 2005) was also computed to identify the dominant scales of variability.

To describe local hydrological phases, a moving-window linear regression was applied to the CDN series with window 95 widths (W) of 12, 36, 60, and 120 months. Within each window, the monthly slope b (in $\sigma \cdot \text{month}^{-1}$) and cumulative change



$\Delta = b \times W$ were calculated. By multiplying Δ by the standard deviation of monthly precipitation (σ_p), results were expressed in millimetres, quantifying the cumulative water volume gained or lost during the corresponding period. Local slopes on the CDN are interpreted as diagnostic descriptors of oscillatory-phase behaviour rather than as permanent statistical trends.

100 3.2 Regime-based interpretation of rainfall variability

The Po river basin, the largest hydrographic system in Italy, provides an illustrative example of these dynamics. SPI1 from 1961 to 2025 (SPI1; Fig. 1a) was analysed to compare the traditional statistical approach with the regime-based perspective offered by the Cumulative Deviation from Normal (CDN; Fig. 1b).

105 Across the full SPI1 record, no statistically significant linear trend was detected, and the Pettitt test identified no significant breakpoints. This indicates the absence of any linear-type rainfall regime shift over the analysed period.

110 Spectral analyses of SPI1 revealed no widespread or persistent periodicities. The significance contours of the wavelet power spectrum (Fig. 1c) show stable periodicities of SPI1 only at scales shorter than 24 months - mostly intermittent - and around 60 months during 2011–2024. Similarly, the Fourier power spectrum of SPI1 (Fig. 1d) exhibits its main peaks at sub-annual scales and a secondary one near 56 months, consistent with the same transient quasi-periodicity identified by the wavelet analysis. On their own, the trend and spectral results support a stationary regime characterized by weak, episodic, and non-persistent periodicities. The CDN (Fig. 1b), however, reveals a clear alternation of wet, dry, and stationary regimes across multiple temporal scales. Its trajectory displays irregular amplitudes and durations, with overlapping phases and non-fixed recurrence, consistent with an intermittently oscillating rather than a cyclic system. For example, distinct wet regimes occurred in 1976–1979, 1991–1997, and 2008–2015, while dry regimes prevailed during 1979–2008 (with intensifications in 115 1988–1992 and 2003–2008) and again in 2021–2023.

The intermittent periodicity highlighted by the wavelet analysis - active at short scales and around 60 months between 2011 and 2024 - finds a clear counterpart in the Figs. 2a, 2c, where regular amplitude and duration of the local oscillations are captured by the 12 and 60-months moving-window regression.

120 From an operational perspective, Fig. 2 illustrates how the moving-window approach allows one to identify precipitation phases, their duration and overlap, and to quantify the corresponding water surplus or deficit. Local slopes of the CDN computed over a window length W are mathematically equivalent to trends derived from SPIW (the W –month SPI), as demonstrated in Appendix S1. As of September 2025, the CDN suggests that, over short time windows (12–36 months), the basin is in a wet regime: the curve is rising, with positive slopes corresponding to a cumulative surplus exceeding ~500 mm over the past three years. At longer scales (60–120 months), a residual negative trend persists - an inheritance of the 125 preceding drought phase - but it is progressively weakening. Taken together, these results suggest moving beyond trends and cycles toward a view of rainfall as a sequence of irregular regimes. In this sense, the CDN bridges the gap between complex spectral tools and the needs of operational climatology, offering a direct way to visualize rainfall as a sequence of alternating regimes rather than noise around a mean.



130

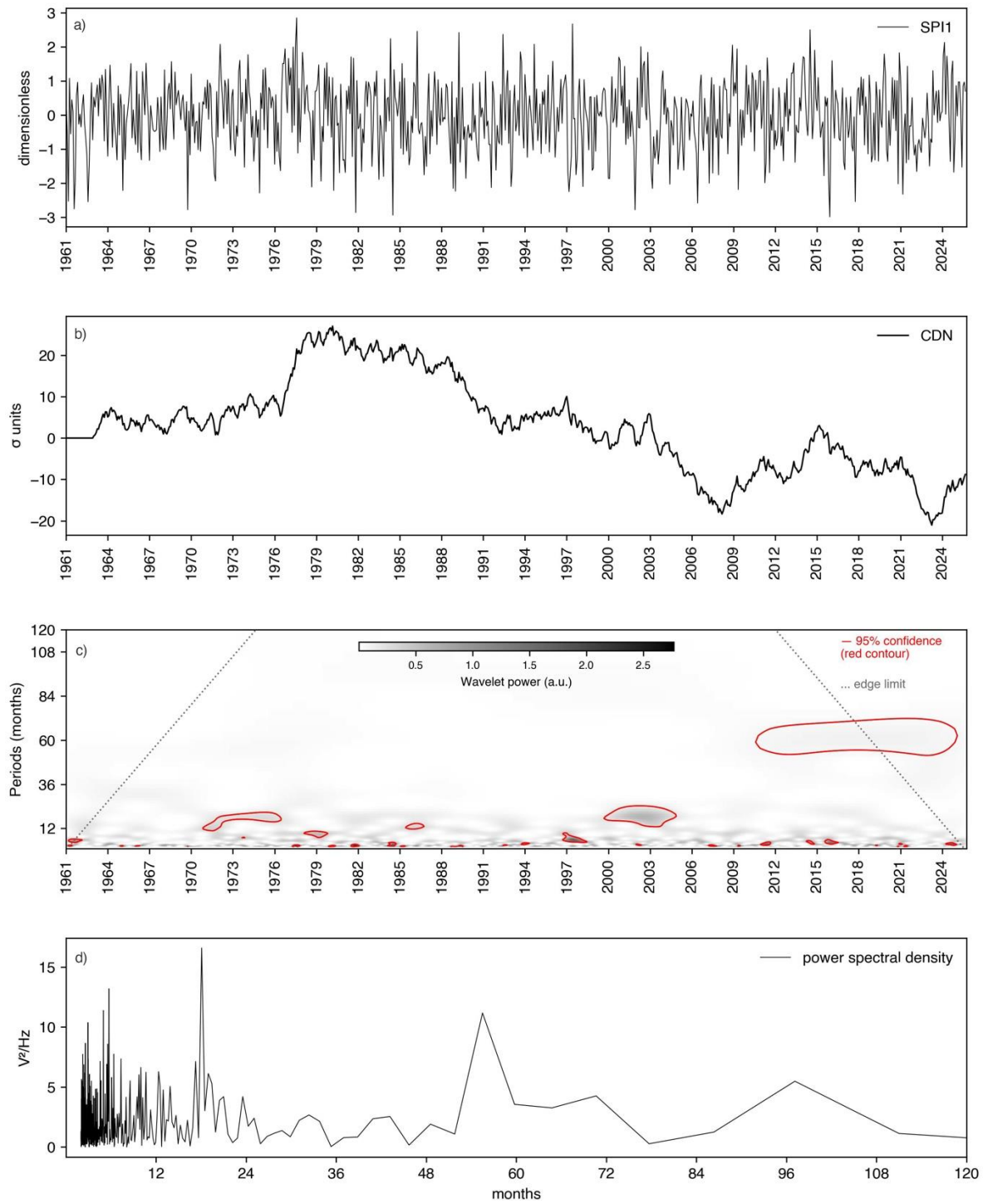




Figure 1: Rainfall variability in the Po River basin. (a) SPI1; (b) CDN of SPI1; (c) wavelet power spectrum (red contours = 95% significance against AR(1) noise) of SPI1; (d) Fourier power density of SPI1.

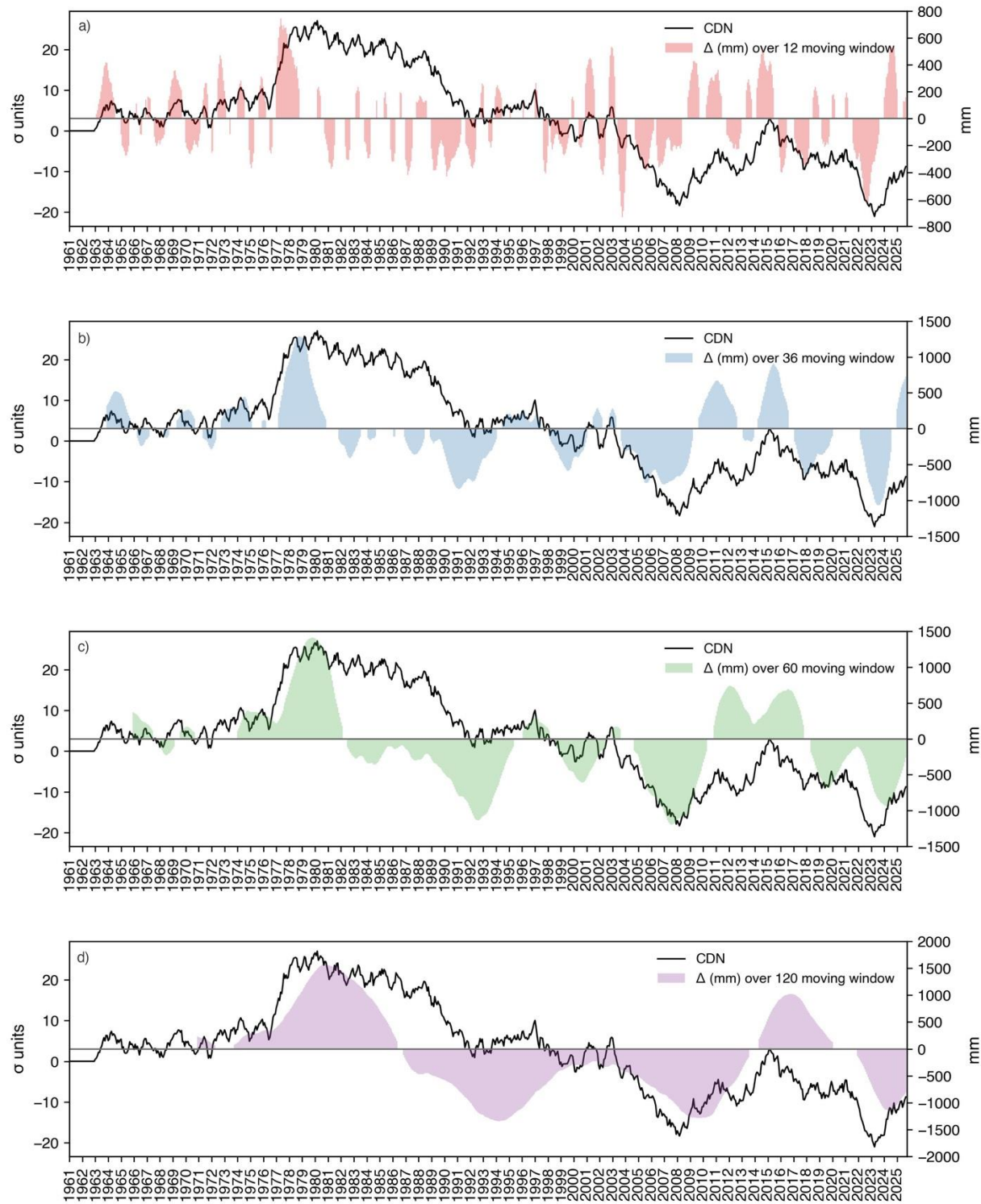




Figure 2: Local trends in the CDN at different moving-window scales. (a-d) CDN (black line, in standard-deviation units) and total change Δ (colored areas) estimated by linear regression over 12-, 36-, 60-, and 120-month windows (b = slope; $\Delta = b \times W$).

Code, data, or code and data availability

140 The analyses rely on standard statistical procedures. Custom scripts used for data processing and figure generation are available from the authors upon reasonable request. Input data are openly available through the ARCIS project at <https://www.arcis.it/wp/en/home-2/>

Author contributions

145 Author Contributions: A.D.P.: Conceptualization, Investigation, Methodology, Visualization, Writing (original draft preparation), Writing (review and editing); M.P. Formal analysis, Validation, Writing (review and editing); R.M.: Validation; Writing (review and editing); S.Q.: Data Curation; Writing (review and editing); E.D.G. Supervision, Formal analysis, Validation, Writing (review and editing).

Competing interests

The authors declare that they have no conflict of interest

150 Disclaimer

Publisher Note: Copernicus Publications remains neutral with regard to jurisdictional claims made in the text, published maps, institutional affiliations, or any other geographical representation in this paper. While Copernicus Publications makes every effort to include appropriate place names, the final responsibility lies with the authors. Views expressed in the text are those of the authors and do not necessarily reflect the views of the publisher.

155 Acknowledgements

The authors thank the ARCIS project for providing open-access precipitation data. The authors acknowledge the use of a large language model (LLM) to assist with English language editing of the manuscript. All scientific content, interpretations, and conclusions remain the sole responsibility of the authors.



Financial support

160 This research received no specific funding.

Review statement

References

165 Beranová, Romana, Radan Huth, e Václav Vít. «A multi-dataset analysis of precipitation trends in Europe». *Journal of Hydrometeorology*, 2025. <https://journals.ametsoc.org/view/journals/hydr/aop/JHM-D-24-0114.1/JHM-D-24-0114.1.xml>.

Caloiero, Tommaso, Paola Caloiero, e Francesco Frustaci. «Long-term Precipitation Trend Analysis in Europe and in the Mediterranean Basin». *Water and Environment Journal* 32, fasc. 3 (2018): 433–45. <https://doi.org/10.1111/wej.12346>.

170

Di Paola, Arianna, Edmondo Di Giuseppe, Ramona Magno, et al. «Building a framework for a synoptic overview of drought». *Science of the Total Environment* 958 (2025): 177949.

175

Dieppois, Bastien, Benjamin Pohl, Julien Crétat, et al. «Southern African Summer-Rainfall Variability, and Its Teleconnections, on Interannual to Interdecadal Timescales in CMIP5 Models». *Climate Dynamics* 53, fasc. 5–6 (2019): 3505–27. <https://doi.org/10.1007/s00382-019-04720-5>.

180

Doane-Solomon, Robert, Tim Woollings, e Isla R. Simpson. «Dynamic Contributions to Recent Observed Wintertime Precipitation Trends in Mediterranean-Type Climate Regions». *Geophysical Research Letters* 52, fasc. 12 (2025): e2024GL114258. <https://doi.org/10.1029/2024GL114258>.

Hu, Zeng-Zhen, e Tsuyoshi Nitta. «Wavelet analysis of summer rainfall over North China and India and SOI using 1891–1992 data». *Journal of the Meteorological Society of Japan. Ser. II* 74, fasc. 6 (1996): 833–44.

185

Kim, Seogyeong, e Kyung-Ja Ha. «Interannual and Decadal Covariabilities in East Asian and Western North Pacific Summer Rainfall for 1979–2016». *Climate Dynamics* 56, fasc. 3–4 (2021): 1017–33. <https://doi.org/10.1007/s00382-020-05517-7>.



Luppichini, Marco, e Monica Bini. «Evolution of rainfall in Italy over the last 200 years: Interactions between climate indices and global warming». *Atmospheric Research* 326 (novembre 2025): 108276.

190 <https://doi.org/10.1016/j.atmosres.2025.108276>.

H. B. Mann, Nonparametric tests against trend. *Econometrica: Journal of the econometric society* 245–259 (1945).

C. Torrence, G. P. Compo, A practical guide to wavelet analysis. *Bulletin of the American Meteorological society* 79, 61–78 (1998).

195 McKee, T.B., Doesken, N.J., Kleist, J., 1993. The relationship of drought frequency and duration to time scales, in: Proceedings of the 8th Conference on Applied Climatology. California, pp. 179–183.

200 Mendes, Maria Paula, Victor Rodriguez-Galiano, e David Aragones. «Evaluating the BFAST method to detect and characterise changing trends in water time series: A case study on the impact of droughts on the Mediterranean climate». *Science of The Total Environment* 846 (2022): 157428.

Pavan, Valentina, Gabriele Antolini, Roberto Barbiero, et al. «High Resolution Climate Precipitation Analysis for North-Central Italy, 1961–2015». *Climate Dynamics* 52, fasc. 5 (2019): 3435–53. <https://doi.org/10.1007/s00382-018-4337-6>

205 Smail, Robert A., Aaron H. Pruitt, Paul D. Mitchell, e Jed B. Colquhoun. «Cumulative deviation from moving mean precipitation as a proxy for groundwater level variation in Wisconsin». *Journal of Hydrology* X 5 (novembre 2019): 100045. <https://doi.org/10.1016/j.jhydrol.2019.100045>.

210 Torrence, Christopher, e Gilbert P. Compo. «A practical guide to wavelet analysis». *Bulletin of the American Meteorological society* 79, fasc. 1 (1998): 61–78.

Truong, Charles, Laurent Oudre, e Nicolas Vayatis. «Selective review of offline change point detection methods». *Signal Processing* 167 (2020): 107299.

215 Valdés-Pineda, Rodrigo, Julio Cañón, e Juan B. Valdés. «Multi-decadal 40-to 60-year cycles of precipitation variability in Chile (South America) and their relationship to the AMO and PDO signals». *Journal of Hydrology* 556 (2018): 1153–70.

220 Vicente-Serrano, Sergio M., Yves Tramblay, Fergus Reig, et al. «High Temporal Variability Not Trend Dominates Mediterranean Precipitation». *Nature* 639, fasc. 8055 (2025): 658–66. <https://doi.org/10.1038/s41586-024-08576-6>.



Weber, Kenneth, e Mark Stewart. «A Critical Analysis of the Cumulative Rainfall Departure Concept». *Ground Water* 42, fasc. 6–7 (2004): 935–38. <https://doi.org/10.1111/j.1745-6584.2004.t01-11-x>.

225 Willems, Patrick. «Multidecadal Oscillatory Behaviour of Rainfall Extremes in Europe». *Climatic Change* 120, fasc. 4 (2013): 931–44. <https://doi.org/10.1007/s10584-013-0837-x>.

Wu, Jiefeng, Xuan Zhang, Gaoxu Wang, Wei Wu, Dejian Zhang, e Tian Lan. «Impacts of hydrometeorological regime shifts on drought Propagation: The meteorological to hydrological perspective». *Journal of Hydrology* 638 (luglio 2024): 131476.

230 <https://doi.org/10.1016/j.jhydrol.2024.131476>.

Youngworth, Richard N., Benjamin B. Gallagher, e Brian L. Stamper. «An overview of power spectral density (PSD) calculations». *Optical manufacturing and testing VI* 5869 (2005): 206–16.

235

Appendix A

We provide a formal proof that the CDN trajectory uniquely determines all multiscale SPI aggregates, reinforcing its role as an integrated descriptor of rainfall regimes. The following steps formalize the statement that the CDN contains all the fundamental information from which every SPI_k derives, and that the CDN acts as a container of the system's multiscale memory. The argument shows that all SPI_k indices depend on K-month sums of SPI1, and that every K-month sum of SPI1 can be written exactly as a difference of the CDN. This is why the CDN captures the multi-year hydrometeorological “phases” (dry or wet regimes), while SPI_k indices quantify how much of that phase is expressed within the specific K-month window.

1. Basic definitions

245 Let

- $t = 1, \dots, T$ be the time index (months), OR $t \in B\{1, \dots, T\}$ be the time index (months) within a period of interest B,
- P_t the basin-averaged precipitation at month t ,
- $m(t) \in \{1, \dots, 12\}$ the calendar month of t ,

For each calendar month m , the 1-month SPI is obtained by fitting a Gamma CDF $G_{1,m}$ on $\{P_t: t \in B, m(t) = m\}$ and then 250 transforming to a standard normal:

$$\text{SPI1}_t \equiv Z_t = \Phi^{-1}(G_{1,m(t)}(P_t)), t = 1, \dots, T. \quad (1)$$



where Φ^{-1} is a function mapping from the probabilistic space of precipitation expressed in mm to the standardized normal space expressed in units of standard deviations.

255 By construction Z_t is approximately standard normal for each m .

2. CDN as cumulative sum of SPI1

Define the Cumulative Deviation from Normal (CDN) as the running sum of SPI1:

$$C_t = \sum_{i=1}^t \text{SPI1}_i = \sum_{i=1}^t Z_i, t = 1, \dots, T \quad (2)$$

260

3. K-month aggregation of SPI1 and relation with CDN

Fix a time scale $K \in \mathbb{N}$, with $K \in \{1, \dots, T\}$. For each $t \geq K$, consider the K-month window $W_{t,K}$ as:

$$W_{t,K} = \{t - K + 1, \dots, t\} \quad (3)$$

265

Then, the sum of SPI1 over the months identified in $W_{t,K}$ is:

$$S_t^{(K)} = \sum_{j=t-K+1}^t \text{SPI1}_j = \sum_{j \in W_{t,K}} Z_j \quad (4)$$

270 Using the definition of C_t , we have the exact identity

$$S_t^{(K)} = (\sum_{i=1}^t Z_i) - (\sum_{i=1}^{t-K} Z_i) = C_t - C_{t-K}, t \geq K \quad (5)$$

Therefore, for every scale K and every time $t \geq K$, the K-month sum of SPI1 is exactly the difference of two CDN values:

275

$$S_t^{(K)} = C_t - C_{t-K} \quad (6)$$

280 This means that the process $\{C_t\}_{t=0, \dots, T}$ uniquely determines all running K-month sums of SPI1 for all K and all t . Eq. (6) shows that any K-month sum of SPI1 is simply the difference between two CDN values, meaning that CDN encodes all temporal scales

4. Connection to K-month SPI indices

The classical K-month SPI (built from raw precipitation P_t) is defined by

$$285 \quad \text{SPI}_K(t) = \Phi^{-1}(G_{K,m(t)}(Q_t^{(K)})) \quad (7)$$



where

$$Q_t^{(K)} = \sum_{i=0}^{K-1} P_{t-i} \quad (8)$$

290

is the K-month cumulative precipitation, and $G_{K,m}$ is the Gamma CDF fitted to $\{Q_t^{(K)} : t \in B, m(t) = m\}$.

Under mild regularity and using the monotonicity of the Gamma and normal transforms, $Q_t^{(K)}$ can be approximated as an affine linear function of $S_t^{(K)}$ and, by substitution of Eq. (6), as a linear function of $(C_t - C_{t-K})$.

$$295 \quad Q_t^{(K)} \approx a_{K,m(t)} + b_{K,m(t)} S_t^{(K)} = a_{K,m(t)} + b_{K,m(t)} (C_t - C_{t-K}) \quad (9)$$

This approximation assumes limited skewness and monotonicity of the transformation; deviations may introduce non-linear effects. So that:

$$300 \quad \text{SPI}_K(t) \approx f_{K,m(t)}(C_t - C_{t-K}) \quad (10)$$

for some monotone linear function $f_{K,m}$ (the composition of the Gamma CDF and the inverse normal, evaluated on an affine function of $C_t - C_{t-K}$). Thus, the CDN not only visualizes regime dynamics but also provides the informational basis for reconstructing SPI_K indices across all scales. In other words, each SPI_K(t) can be viewed as a monotone transformation of a 305 quantity $S_t^{(K)}$ that depends only on the CDN via $C_t - C_{t-K}$.

Assumptions and Limitations

The derivation assumes stationarity within the calibration period, monotonicity of the Gamma and normal transforms, and negligible zero-inflation. Strong departures from these conditions may affect the linear approximation in Eq. (9).

310